

PHYSICAL REVIEW B **89**, 195120 (2014)**Topological insulators with arbitrarily tunable entanglement**J. C. Budich,^{1,2,3} J. Eisert,⁴ and E. J. Bergholtz⁴¹*Department of Physics, Stockholm University, SE-106 91 Stockholm, Sweden*²*Institute for Theoretical Physics, University of Innsbruck, 6020 Innsbruck, Austria*³*Institute for Quantum Optics and Quantum Information, Austrian Academy of Sciences, 6020 Innsbruck, Austria*⁴*Dahlem Center for Complex Quantum Systems, Freie Universität Berlin, Arnimallee 14, 14195 Berlin, Germany*

(Received 21 November 2013; revised manuscript received 29 April 2014; published 15 May 2014)

We elucidate how Chern and topological insulators fulfill an area law for the entanglement entropy. By explicit construction of a family of lattice Hamiltonians, we are able to demonstrate that the area law contribution can be tuned to an arbitrarily small value but is topologically protected from vanishing exactly. We prove this by introducing novel methods to bound entanglement entropies from correlations using perturbation bounds, drawing intuition from ideas of quantum information theory. This rigorous approach is complemented by an intuitive understanding in terms of entanglement edge states. These insights have a number of important consequences: The area law has no universal component, no matter how small, and the entanglement scaling cannot be used as a faithful diagnostic of topological insulators. This holds for all Renyi entropies which uniquely determine the entanglement spectrum, which is hence also nonuniversal. The existence of arbitrarily weakly entangled topological insulators furthermore opens up possibilities of devising correlated topological phases in which the entanglement entropy is small and which are thereby numerically tractable, specifically in tensor network approaches.

DOI: [10.1103/PhysRevB.89.195120](https://doi.org/10.1103/PhysRevB.89.195120)

PACS number(s): 73.20.-r, 03.65.Vf, 03.67.Bg, 03.67.Mn

I. INTRODUCTION AND KEY RESULTS

Since the experimental discovery [1,2] and first theoretical explanation [3–5] of the quantum Hall effect, topological phenomena have triggered some of the most active and intriguing research fields in physics. An important milestone in the theoretical understanding of topological phases has been reached with the notion of topological order [6] as a means to distinguish phases of matter beyond the paradigm of local order parameters associated with spontaneous symmetry breaking [7]. In parallel, the entanglement entropy, which measures the amount of quantum correlation between a system and its environment as a function of the boundary “area” L , has developed as a standard tool in quantum many-body physics, providing important insights into properties of a wide range of physical systems [8]. Notably, it can be used to distinguish, sometimes even classify, different phases of matter, thus providing insights that are valuable, e.g., in the context of numerical simulations [9].

More recently, the notions of entanglement scaling and topological phases have been bridged, showing that there is a topological contribution γ to the entanglement entropy of a bipartite system that is unique to topologically ordered phases. This scale-invariant term has been coined *topological entanglement entropy* (TEE) and depends only on the logarithm of the total quantum dimension of the topological phase [10–13]. Putting together these concepts, the generic scaling of the entanglement entropy in two spatial dimensions (2D) reads

$$S(L) = \alpha L - \gamma + O(1/L) \quad (1)$$

for a suitable $\alpha \geq 0$. However, the whole family of integer quantum Hall states [1,3,4] has quantum dimension 1, implying a vanishing TEE γ . Still, integer quantum Hall states and their lattice translation-invariant analogs called *Chern insulators* (CIs) [14] are gapped topological phases that are not characterized by any conventional local order and cannot be

adiabatically connected to trivial insulators. In fact, according to the definition suggested in Ref. [15], the CIs belong to the class of topologically ordered systems.

In this work, we pose the natural and important question of to what extent the topological nature of CI states and topological insulators in 2D [16–18] can be inferred from their entanglement scaling and, more generally, entanglement spectra. Our analysis, expected to generalize to all standard topological insulator classes [19–21] with spatial dimension $d > 1$, is rooted in the following observations. The area law stems from two qualitatively different contributions: a trivial contribution and a topological one. The topological part is in one-to-one correspondence with the topologically protected edge states occurring at the boundary of a CI (Fig. 1). This contribution may be considered a fingerprint of the nonvanishing Chern number in the sense that its value will be nonzero for any state that is adiabatically connected to a nontrivial CI. Remarkably, however, we find that there is no nonzero lower bound, which might have been expected in analogy with the lowest Landau level, which is a Chern insulator enjoying minimum fluctuations in the (guiding center) coordinates which fail to commute, $[X, Y] = i\ell_B^2$, when projected to the band. In contrast, the trivial part can be adiabatically tuned to zero just as the entire entanglement can be tuned to zero for trivial insulators in the atomic limit. In order to alter both contributions simultaneously, we devise a construction of a Chern insulator model built via “dimensional extension” [22,23] of a topologically nontrivial one-dimensional (1D) model. We are able to demonstrate that no lower bound can be put on α even for a CI state and that it has no even arbitrarily small universal component. The local correlations can be chosen arbitrarily close to those of uncorrelated Slater determinants. In fact, this is true for the whole family of so-called Renyi entropies, $S_p(L)$, each having a scaling of the form of Eq. (1). The collection of (integer) Renyi entropies fully determines

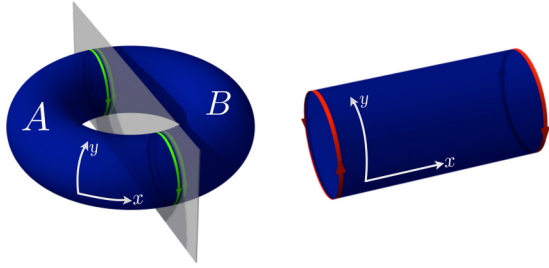


FIG. 1. (Color online) Sketch of our setup and the bulk-boundary correspondence in Chern insulators. Bipartitioning the system into distinct regions (A and B) on a torus gives rise to virtual edge states (green) in the entanglement Hamiltonian which are close analogs of the physical edge states (red) on a cylinder.

the entanglement spectrum [24], and our results imply that even this more complete information does not contain truly universal information beyond the fingerprint mentioned above.

In order to prove this we introduce rigorous methods of upper bounding entanglement entropies in terms of *correlations* only, using perturbation bounds on spectra of fermionic correlation matrices and instruments from harmonic analysis. On an intuitive level, we show that the contribution to α depends on the steepness of the dispersion of the edge states in a sample with fixed boundaries. This intuition is guided by the insight that the bulk entanglement spectrum [24] is typically closely related to the gapless excitations at the edge of a topological state [24,25]. The possibility of arbitrarily suppressing the area law coefficient may be useful for the construction of representatives of correlated topological phases like fractional Chern insulators [26–30], specifically with tensor network methods where the prefactor of the area law relates to the required bond dimension.

The remainder of this paper is organized as follows: in Sec. II, we generally discuss entanglement properties of free fermionic systems with a focus on the relation between topological edge states and the area law coefficient of the entanglement scaling. Building on this general analysis, a family of Chern insulators with arbitrarily tunable entanglement is constructed in Sec. III. Upper and lower bounds on the Renyi entanglement entropies of this model family are obtained from rigorous analytical methods introduced in this work (for details see the Appendix) and are confirmed by extensive numerical analysis. Finally, we present a concluding discussion in Sec. IV.

II. ENTANGLEMENT IN FREE FERMIONIC SYSTEMS

A. Two-band fermionic systems and entanglement

Hamiltonians

The CI models we are considering are noninteracting gapped two-band fermionic systems with no pairing terms. For two-dimensional cubic lattices with $L \times L$ sites on a torus, such a Hamiltonian takes the form

$$H = \sum_{I,J} c_I^\dagger h_{I,J} c_J, \quad (2)$$

where the fermionic modes are labeled by $I = (j, k, \uparrow)$ for $j, k = 1, \dots, L$. Their ground states are Slater determinants

of all single-particle states below the energy gap. When the system is divided into two subsystems A and B by virtue of a cut in real space (Fig. 1), the reduced state of the individual subsystems generically exhibits a nonzero entanglement entropy. Ground states ρ of such models are always fermionic Gaussian states. This implies that the reduced density matrix ρ_A for subsystem A can be viewed as a free fermionic thermal state with unit inverse temperature of the isolated subsystem A , i.e.,

$$\rho_A = e^{-H_E} / \text{tr}(e^{-H_E}), \quad (3)$$

where the *entanglement Hamiltonian* H_E is again quadratic in the fermionic operators. For such free fermionic models the ground state ρ is defined by the Hermitian, positive correlation matrix C , with entries

$$C_{I,J} = \text{tr}(\rho c_I^\dagger c_J). \quad (4)$$

H_E is determined in terms of the truncated correlation matrix, $C^{(A)}$, the submatrix of C associated with indices only in A . If $\{\xi_j\}$ denotes the set of eigenvalues of $C^{(A)}$ and $\{\epsilon_j\}$ denotes the set of single-particle entanglement energies, the relation reads, for all j [31],

$$\epsilon_j = \log(1 - \xi_j) \xi_j^{-1}. \quad (5)$$

B. Entanglement entropies

In momentum space, the Hamiltonians become

$$H = \sum_{\mathbf{k}} (f_\uparrow^\dagger(\mathbf{k}), f_\downarrow^\dagger(\mathbf{k})) h(\mathbf{k}) \begin{pmatrix} f_\uparrow(\mathbf{k}) \\ f_\downarrow(\mathbf{k}) \end{pmatrix}, \quad (6)$$

where $\mathbf{k} = (k_x, k_y)$,

$$h(\mathbf{k}) = \sum_{j=1}^3 d_j(\mathbf{k}) \sigma_j, \quad (7)$$

and $\sigma_1, \sigma_2, \sigma_3$ are the Pauli matrices. The wave vectors take the values $k_x, k_y = 2\pi l/L \in (-\pi, \pi]$ for $l = -L/2 + 1, \dots, L/2$ (we also allow for $L_x \times L_y$ lattices). The two energy bands are separated by $\pm \|\mathbf{d}(\mathbf{k})\|$. For a fully occupied lower band and unoccupied upper band, the correlation matrix in momentum space of the ground state is

$$\bar{C} = \bigoplus_{\mathbf{k}} \frac{1}{2} \left(\mathbb{1} - \sum_{j=1}^3 \frac{d_j(\mathbf{k})}{\|\mathbf{d}\|} \sigma_j \right). \quad (8)$$

Given the toroidal symmetry of the problem, when computing the entanglement entropy, we keep the momentum space along the k_y direction but turn to real space otherwise [32,33]. The fermionic operators are then transformed as

$$f_\uparrow(\mathbf{k}) = \sum_{l=1}^L e^{-ik_x l} c_{l,\uparrow}(k_y) / L^{1/2}. \quad (9)$$

The ground state of each decoupled Hamiltonian labeled by k_y is associated with a correlation matrix $C(k_y)$ in real space. We allow for arbitrary Renyi entanglement entropies S_p , $p \geq 1$, the standard von Neumann entropy being recovered in the limit $p \downarrow 1$. Indeed, it is known that all integer Renyi entropies uniquely determine the entire entanglement spectrum. Hence, our study allows us to conclude that the entanglement spectrum

is also nonuniversal. The entanglement entropy S_p decouples into a sum over the contributions for each k_y . In this bipartition, only submatrices of the correlation matrix with both indices in A contribute. Denote with $C^{(A)}(k_y)$ the submatrix of $C(k_y)$ corresponding to sites contained in A , with eigenvalues $\{\xi_j(C^{(A)}(k_y))\}$. Then, defining

$$h_p(x) = \log_2[x^p + (1-x)^p]/(1-p), \quad (10)$$

the expression for the Renyi entanglement entropy takes the form

$$S_p(L) = \sum_{k_y} \sum_j h_p(\xi_j(C^{(A)}(k_y))). \quad (11)$$

C. Analogy with edge states of a cylinder

To get a physical intuition for the situation at hand, it is helpful to consider $Q = \mathbb{1}/2 - C$. It can be interpreted as a Hamiltonian with the same eigenstates as the original system but with flat bands, i.e., $\epsilon_- = -1/2$ for all occupied states and $\epsilon_+ = 1/2$ for all empty states [19,34–38]. Equation (5) implies that the truncated flat-band Hamiltonian $Q^{(A)} = \mathbb{1}/2 - C^{(A)}$ is related to the entanglement Hamiltonian as

$$H_E = 2\text{arctanh}(2Q^{(A)}) \quad (12)$$

[34,39]. It is thus clear that H_E and the physical Hamiltonian H must have similar properties regarding topologically protected edge states: Q results from H via adiabatic deformation and is hence topologically equivalent to the physical Hamiltonian. H_E is related to $Q^{(A)}$ via a monotonous mapping of its spectrum.

The area law character of edge-mode contributions to the entanglement entropy can be intuitively understood considering a cylinder geometry where the cut is translation invariant in the y direction. A chiral edge state of H_E is then described by an energy dispersion ϵ_e of the momentum k_y along the cut crossing the energy gap. The number of low-lying entanglement levels associated with that edge state grows linearly with the length of the cut L . The quantized L wave vectors k_y are equidistant so that the number of states in the edge-mode dispersion satisfying $\epsilon_e(k_y) < \epsilon_c$ grows linearly with L for an arbitrary cutoff $\epsilon_c > 0$. Hence, a chiral edge mode results in a nonvanishing area law for the entanglement entropy, i.e., $S_p \geq \alpha L$ for some $\alpha > 0$. The expected α contributed by the chiral edge mode can be made plausible at this simple level (for a rigorous treatment, see below): If the edge state dispersion is steep, ϵ_e will cross the gap rapidly as a function of k_y , resulting in only a small fraction of its L levels having low energies. A steep edge dispersion hence implies little entanglement.

III. CHERN INSULATORS WITH TUNABLE AREA LAW

A. Model building

We now construct a family of CI states with Chern number 1 in which the steepness of the edge states along with the coefficient α of the area law can be tuned by a single parameter μ . To this end we proceed in three steps. First, we discuss the entanglement scaling of a well-known Dirac model for a CI [21,23] from a viewpoint of dimensional extension. Second, we introduce a means to tune the topological edge-state

contribution to the area law to an arbitrary value. Third, we show how to get rid of the nontopological contribution to the entanglement which otherwise masks the edge-state contribution. Our analysis is inspired by the fact that 2D CI states can be obtained by dimensional extension [22,23] of particle-hole symmetry (PHS) preserving topologically nontrivial 1D band structures [23,40,41]. In our case, k_y , the momentum variable along the cut, plays the role of the additional coordinate of the dimensional extension. At $k_y = 0$ we define a 1D model as

$$h(k_x, k_y = 0) = \sin(k_x)\sigma_2 - \cos(k_x)\sigma_3 \quad (13)$$

in Eq. (6). This 1D model is topologically characterized by a quantized Zak-Berry phase [42] of π which is protected by the PHS $\mathcal{C} = \sigma_1 K$ [43], where K denotes complex conjugation. An interpolation with Chern number 1 between Eq. (13) and the trivial 1D model $h(k_x, k_y = \pm\pi) = \sin(k_x)\sigma_2 + [2 - \cos(k_x)]\sigma_3$ is given by the Dirac model for a CI [23], i.e.,

$$h(k_x, k_y) = -\sin(k_y)\sigma_1 + \sin(k_x)\sigma_2 + [1 - \cos(k_y) - \cos(k_x)]\sigma_3. \quad (14)$$

The nature of the edge states may be understood from the dimensional extension: The 1D model at $k_y = 0$ supports a single pair of zero-energy end states, while the trivial model at $k_y = \pm\pi$ does not have any subgap states. During the gapped interpolation, these zero modes must hence be gapped out continuously, which gives rise to a single chiral edge mode crossing the gap of the 2D model with fixed boundary conditions.

To arrive at a model with tunable entanglement entropy, we replace the $\sin(k_y)$ and $\cos(k_y)$ functions in Eq. (14) by the C^∞ functions $s_\mu, c_\mu : (-\pi, \pi] \rightarrow \mathbb{R}$,

$$s_\mu(k_y) = \begin{cases} \text{sgn}(k_y)e^{-k_y^2 - (|k_y| - \mu)^{-2} + 8/\mu^2}, & |k_y| < \mu, \\ 0, & \mu < |k_y| < \pi, \end{cases} \quad (15)$$

$$c_\mu(k_y) = \begin{cases} [1 - s_\mu(k_y)^2]^{1/2}, & |k_y| < \mu/2, \\ -[1 - s_\mu(k_y)^2]^{1/2}, & |k_y| > \mu/2, \end{cases} \quad (16)$$

where $\mu \in (0, \pi]$ is a real parameter and s_μ, c_μ are 2π periodically continued outside of the interval $(-\pi, \pi]$ to formally define a lattice model with unit lattice constant. These functions satisfy $s_\mu^2 + c_\mu^2 = 1$ and have the same behavior under parity as \sin and \cos , respectively. The substitution of $\sin(k_y)$ by $s_\mu(k_y)$ and $\cos(k_y)$ by $c_\mu(k_y)$ does not change the instantaneous 1D models at $k_y = 0$ and $k_y = \pm\pi$. This modified model represents a smooth interpolation between the same 1D models and still has Chern number 1. However, the Hamiltonian depends on k_y only in the tunable interval $(0, \mu]$. Following our previous line of argumentation, the edge-state contribution to the area law coefficient α hence becomes arbitrarily small for small μ . However, the trivial 1D model $h(k_x, |k_y| > \mu) = \sin(k_x)\sigma_2 + [2 - \cos(k_x)]\sigma_3$ still gives a nontopological contribution to the area law due to its dependence on k_x that gives rise to delocalized states. As a final step, we introduce a slightly modified dimensional extension, still with Chern number 1, to the k_x -independent trivial 1D

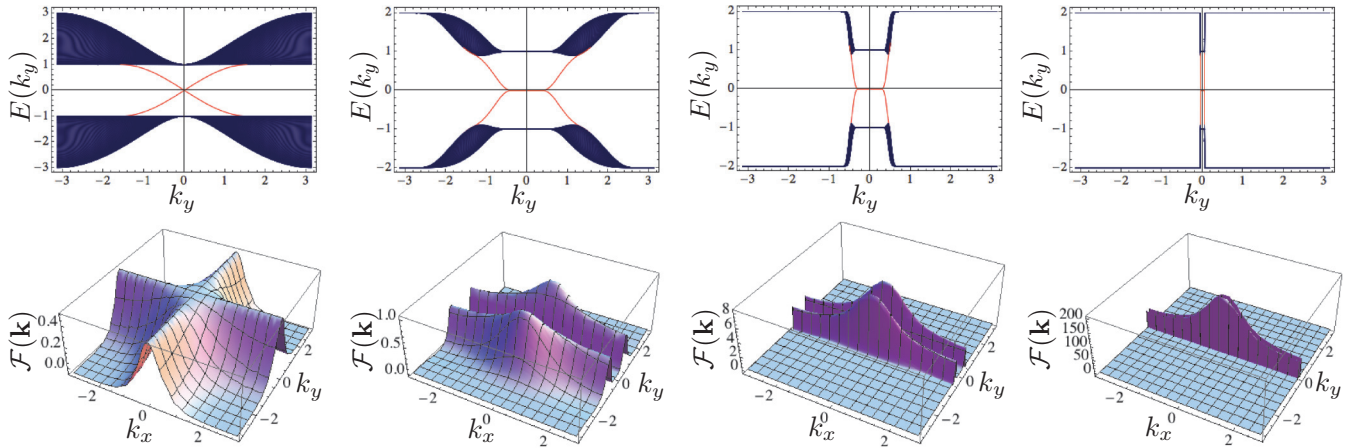


FIG. 2. (Color online) Band structure and Berry curvature. The top row shows the energy dispersion as a function of the transverse momentum k_y in the model defined on a cylinder serving as an analogy, and the bottom row shows the corresponding Berry curvature distribution \mathcal{F} for the model on the torus. From the left to right, the data are displayed for the standard Dirac model (14) and our model (17), with $\mu = \pi, 1, 0.2$, respectively. For small values of $\mu > 0$, the Berry curvature is strongly peaked around $k_y = \pm\mu/2$, which is necessary to maintain a unit Chern number, $C = \int_{\text{BZ}} \mathcal{F}(\mathbf{k}) d^2k / (2\pi)$. The edge states exhibit a very steep slope around $k_y = \pm\mu/2$ and a plateau of width μ at zero energy between $k_y = -\mu/2$ and $k_y = \mu/2$.

model $\tilde{h}_\mu(k_x, |k_y| > \mu) = 2\sigma_3$ by defining

$$\begin{aligned} \tilde{h}_\mu(k_x, k_y) = & s_\mu(k_y)\sigma_1 + \frac{1}{2}[1 + c_\mu(k_y)]\sin(k_x)\sigma_2 \\ & + \{1 - c_\mu(k_y) - \frac{1}{2}[1 + c_\mu(k_y)]\cos(k_x)\}\sigma_3. \end{aligned} \quad (17)$$

The CI model (17) is equal to the atomic insulator $h_0(k_x, k_y) = 2\sigma_3$ for $|k_y| > \mu$ and is the key model for which we will demonstrate the tunability of the entanglement entropy.

To further elucidate the properties of (17), we compare the energy spectra on (long) cylinders as well as the Berry curvatures for a conventional Dirac model (14) and our family of CI Hamiltonians (17) in Fig. 2. For small values of μ , the Berry curvature is strongly peaked around $k_y = \pm\mu/2$. The edge states exhibit a very steep slope around $k_y = \pm\mu/2$ and a plateau of width μ at zero energy between $k_y = -\mu/2$ and $k_y = \mu/2$, which turns out to give the main contribution to the entanglement entropy. However, the whole range of low-energy states as a function of k_y decreases linearly with μ for small μ , and we hence expect the area law coefficient α of the entanglement entropy to do so as well, as confirmed by our numerical analysis (see Fig. 3) and in compliance with the analytical bounds, to which we turn next.

B. Upper and lower bounds to entanglement entropies

To assess that question analytically, we introduce a versatile tool to bound entanglement entropies, allowing us to show that ground states of free fermionic systems for which correlations decay sufficiently rapidly exhibit very little entanglement entropy. We first state the general result applied to a 1D system of length L , but it will be clear how to apply it to the above decoupled 2D situation. If $C(k_y)$ is the correlation matrix of a translationally invariant pure state, we say it decays with power $\beta > 0$ whenever there exists a $c > 0$ such that

$$|C(k_y)_{j,k}| \leq cd(j,k)^{-\beta}, \quad (18)$$

where d is the distance in the lattice with periodic boundary conditions. For each k_y individually, one can then show the validity of an area law,

$$S_p(k_y) \leq cc_\beta, \quad (19)$$

where $c_\beta > 0$ is a constant depending on β only and c is the constant of Eq. (18): We find that $\beta > 2$ is in fact sufficient to prove the validity of an area law in free fermionic models (for details, see the Appendix). The proof idea is to decompose the correlation matrix $C(k_y)$ for each k_y into

$$C(k_y) = C^{(AB)}(k_y) + M(k_y), \quad (20)$$

where $C^{(AB)}(k_y)$ captures the uncorrelated situation between A and its complement reflected by no entanglement at all. Then, one can use Weyl's perturbation theorem [44] to bound the extent to which each of the eigenvalues of $C(k_y)$ may be different from those of $M(k_y)$, a correlation matrix reflecting a product state. From a counting of the respective eigenvalues

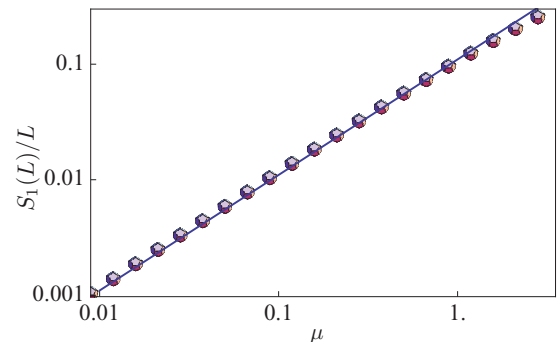


FIG. 3. (Color online) Entanglement area law manifested in the large L limit of $S_1(L)/L$ as a function of μ on a log-log scale. For sufficiently small μ , the numerically obtained values of $S_1(L)/L$ are proportional to μ to an extraordinary precision, confirming our conclusion that $\lim_{L \rightarrow \infty} S_1(L)/L \rightarrow 0$ as $\mu \downarrow 0$. The blue line for 0.11μ is included as a guide to the eye.

and bounds to their magnitude, one arrives at a bound to $S_p(k_y)$ from knowledge about the decay of correlations alone.

What remains to be seen is how one can derive the decay behavior of Eq. (18) from the given dispersion relation of the model. Here, an elegant tool comes into play, using the machinery of harmonic analysis: The decay of correlations is obtained from a suitable Fourier series of the dispersion relation. One can derive such a decay, however, purely from knowledge about derivatives of the dispersion relation: c is obtained from integrals over absolute values of third derivatives of dispersion relations. In this way, one arrives at the result with little computation, albeit in a fully rigorous way: It is clear from the dispersion relation of our model (17) that these integrals over third derivatives can be made arbitrarily small (for details, see the Appendix). Intuitively put, we hence make use of the freedom to appropriately tune the correlation decay in real space by altering the physical model to our desire, while keeping the topological features intact.

Observation 1. Very low entanglement in Chern insulators. For any $\alpha > 0$ and any $p \geq 1$, there are two-band Chern insulator models on $L \times L$ tori, $L \geq L_0$, L_0 chosen sufficiently large, such that the entanglement entropy of the bisected system satisfies

$$S_p(L) \leq \alpha L. \quad (21)$$

For this to be valid, one merely has to pick sufficiently small $\mu > 0$, as α will be monotonously decreasing with μ and will approach zero. Since in the partially decoupled situation one can lower bound the entanglement entropy of each 1D system by a continuous function $k_y \mapsto f(k_y)$ for the translationally invariant gapped models considered here, it is easy to see that in the thermodynamic limit $L \rightarrow \infty$ and with a concomitant refinement in momentum space, the entanglement entropy has to grow linearly in L , unless the ground state is obtained for a trivial, \mathbf{k} -independent, model with constant \mathbf{d} . Such a state is, however, topologically trivial and separated from any Chern insulator by a closing of the bulk gap.

Observation 2. Nontrivial area laws in Chern insulators. For any two-band Chern insulator model on $L \times L$ tori and any $p \geq 1$, there exists an $\alpha > 0$ and an L_0 such that the entanglement entropy of the bisected system satisfies $S_p(L) \geq \alpha L$ for $L \geq L_0$.

C. Numerical analysis

To complement the analytical considerations, we have performed an extensive numerical analysis which we briefly report here. All of our numerical results are fully consistent with the rigorous results and also confirm that the actual entanglement boundary scales similarly with μ as the analytical bound does in the limit of large systems sizes. In particular, for small μ and large L we find that $S_1(L)/L$ is indeed directly proportional to μ to very high precision, as is illustrated in Fig. 3 for $L = 60\,000$ [45].

IV. CONCLUSIONS AND DISCUSSION

We have demonstrated the close correspondence between the area law entanglement scaling of topological insulators in two dimensions and their topologically protected edge states. In particular, we have shown that the entanglement

entropy over a cut, while being topologically protected from assuming the value zero, is nonuniversal and, in fact, arbitrarily tunable. While the analysis focused on a model with broken time-reversal symmetry and Chern number $C = 1$, our construction immediately generalizes to models with arbitrary Chern numbers and to time-reversal-symmetric \mathbb{Z}_2 topological insulators in 2D: Models with arbitrary Chern numbers are obtained by $k_x \mapsto Nk_x$, with integer N , which directly leads to $C \mapsto NC$ and $S_p(L) \mapsto NS_p(L)$. A time-reversal-symmetric \mathbb{Z}_2 topological insulator with tunable entanglement consists of two time-reversed copies of our model in Eq. (17). We also find that our analysis can be generalized to higher dimensions.

For the particular case of symmetry-protected topological states in 1D systems, there is a finite lower bound to the entanglement entropy. Co-occurring with our work, Ref. [46] independently concluded that the entanglement spectrum of Chern insulators is nonuniversal using very different means. In our rigorous framework, this is natural as each Renyi entropy has been explicitly proven to be nonuniversal, and taken together, the (integer) Renyi entropies uniquely determine the complete entanglement spectrum. It is common practice to infer topological properties for counting the number of low-lying ‘‘entanglement energies’’ as a function of the transverse momentum and comparing this number with predictions from conformal field theory. In our model the entanglement is ‘switched off’ at an arbitrarily chosen transverse momentum, thus inferring the topology of the ground state in this fashion is impossible in any finite-size numerical investigation.

Our results have notable implications for numerics in the context of tensor-network approaches to Chern insulators [47–49]. In particular, our finding that topological phases can have very low entanglement is encouraging for the simulation of interacting topological phases using entanglement-based approaches. Although the weakly entangled topological insulators introduced here have a peaked Berry curvature, it is becoming increasingly clear that interesting strongly correlated phases can exist far beyond the idealized Landau level situation with a constant Berry curvature [30]. Having a lattice model with a tunable Berry curvature while maintaining a sizable band gap is likely to bring new insights. We hope our results stimulate such further work.

ACKNOWLEDGMENTS

We thank E. Ardonne, D. Haldane, and M. Hermanns for inspiring discussions and R. Thomale and P. Zanardi for comments. J.C.B. was sponsored by the Swedish Research Council (VR) and the ERC Synergy Grant UQUAM, J.E. by the EU (SIQS, RAQUEL, COST), the ERC (TAQ), the FQXi, and the BMBF (QuOReP), and E.J.B. is supported by the Emmy Noether program (BE 5233/1-1) of the DFG.

APPENDIX

In this Appendix, we discuss the methods used in order to formulate the results presented in the main text. The material presented here is not needed in order to understand the conclusions of the main text. Since new techniques are introduced here, however, we present them in great detail. We also present a figure that provides further intuition to the argument.

1. Upper bounds for entanglement entropies

We here introduce a method to upper bound entanglement entropies in translationally invariant 1D free fermionic systems of L_x sites, with L_x being even for simplicity of notation. This argument is built upon statements linking correlations to entanglement entropies in free bosonic systems [50] or in general spin models, where an exponential decay of correlations is required [51]. Here, a slow algebraic decay is sufficient.

The basic idea is to decompose the correlation matrix into one part of a direct sum of parts relating to A and its complement, from which the entanglement entropy can be computed, and a second remaining part that reflects the quickly decaying correlations. Naive bounds on this remaining part will not be sufficient. Weyl’s perturbation theorem [44], however, will be the instrument that allows us to capture the decay and the precise number of spectral values of this remaining part. This argument is expected to be of use also in other contexts where block-Toeplitz methods [52] are inapplicable or too tedious. The $2L_x \times 2L_x$ circulant correlation matrix is denoted by C . Again, we say it decays with power $\beta > 0$ whenever there exists a $c > 1$ such that

$$|C_{j,k}| \leq cd(j,k)^{-\beta}, \tag{A1}$$

where d is the distance in the lattice with periodic boundary conditions. Of course, this is true in particular if the correlations decay exponentially with the distance. For generality, we consider arbitrary Renyi entropies S_p with $p \geq 1$, with $S_1 = S$ being the standard von Neumann entropy. Again, as is well known, all positive-integer Renyi entropies uniquely specify the entire entanglement spectrum.

Theorem 1. Upper bounds to entanglement entropies. Consider the ground state of a free fermionic translationally invariant two-band system of even length L_x , with a filled lower band and empty upper band, with correlations decaying as in Eq. (A1). If $\beta > 2$, then each (Renyi) entanglement entropy satisfies the area law $S_p \leq cc_\beta$ for a suitable constant $c_\beta > 0$.

Proof. The latter constant c_β does not depend on the system size. Denote with ξ_j^\downarrow the j th eigenvalue of a matrix in nonincreasing order. Denote with $C^{(AB)}$ the submatrix of C that is obtained from C by the pinching for which all correlations between A and the complement B vanish. Since the state is pure, the spectra of the submatrices associated with A and its complement will be identical, and hence the (Renyi) entanglement entropy can for any $p \geq 1$ be written as

$$S_p = \sum_{j=1}^{2L_x} h_p(\xi_j^\downarrow(C^{(AB)})) \tag{A2}$$

in terms of the family of entropy functions $h_p : [0, 1] \rightarrow [0, 1]$ defined as

$$h_p(x) = \frac{1}{1-p} \{\log_2[x^p + (1-x)^p]\}. \tag{A3}$$

The first and key step will be a consequence of proper use of Weyl’s perturbation theorem [44]. Since the ground state is unique and a pure state, the spectral values are all contained

in $\{1, 0\}$, that is,

$$\xi_j^\downarrow(C) = 1 \tag{A4}$$

for $j = 1, \dots, L_x$ and

$$\xi_j^\downarrow(C) = 0 \tag{A5}$$

for $j = L_x + 1, \dots, 2L_x$: This reflects the lower band being filled and the upper being empty. The remaining part is referred to as M , so that

$$C = C^{(AB)} + M. \tag{A6}$$

M reflects the decaying correlations in the ground state. We now make use of Weyl’s perturbation theorem: We find for the largest L_x (twice degenerate) eigenvalues of $C^{(AB)}$

$$1 - \xi_j^\downarrow(C^{(AB)}) \leq \xi_j^\downarrow(M), \quad j = 1, \dots, L_x, \tag{A7}$$

and for the smallest eigenvalues

$$\xi_j^\downarrow(C^{(AB)}) \leq \xi_{j-L_x}^\downarrow(M), \quad j = L_x + 1, \dots, 2L_x. \tag{A8}$$

That is to say, both the large eigenvalues close to 1 and the small ones close to 0 are only slightly perturbed by the same eigenvalues of M . This implies that, using the monotonicity of h on $[0, 1/2]$,

$$\begin{aligned} S_p &= \sum_{j=1}^{L_x} h_p(\xi_j^\downarrow(C^{(AB)})) + \sum_{j=L_x+1}^{2L_x} h_p(\xi_j^\downarrow(C^{(AB)})) \\ &\leq 2 \sum_{j=1}^{L_x} h_p(\xi_j^\downarrow(M)). \end{aligned} \tag{A9}$$

We now again employ Weyl’s perturbation theorem, except now to M : We hence reveal the structure of eigenvalues of M , which rapidly decay in the same way as the correlation matrix entries decay. Acknowledging that for each of the four subblocks of M one encounters rapidly decaying correlations and using that $h_p(1/2) = 1$ is the maximum value of the entropy function, one finds

$$S_p \leq 8 \sum_{j=1}^{\infty} h_p(\min(jc_j^{-\beta}, 1/2)), \tag{A10}$$

again giving rise to an upper bound by extending the sum to L_x by 1 to ∞ . We now use that

$$h_p(cx) \leq \max(1, p)ch_p(x) \tag{A11}$$

for all $c > 1$ and all $x \in [0, 1]$ such that $cx \in [0, 1]$. What is more, it is easy to see that

$$\log(1+x) \leq x \tag{A12}$$

for $x > 0$. This means that

$$S_p \leq 8 \max(1, p)c \sum_{j=1}^{\infty} h_p(j^{1-\beta}) =: cc_{p,\beta} \tag{A13}$$

for a suitable $c_{p,\beta} > 0$, when $\beta > 2$, as the infinite sum then converges for $p \geq 1$. This can easily be seen using Eq. (A12), employing the fact that

$$\sum_{j=1}^{\infty} j^{-(\beta-1)p} < \infty \tag{A14}$$

whenever $(\beta - 1)p > 1$.

Note that the same argument is also applicable for any number of bands and is stated for a two-band model merely for simplicity of notation. The above proof is generally still valid as is, with the only modification being that the prefactor will linearly grow with the number of bands considered.

2. Harmonic analysis and correlation decay

The actual decay behavior of the correlations can here be determined using tools of harmonic analysis [53].

Lemma 1. Fourier components [53]. Let $\tilde{f} : \mathbb{R} \rightarrow \mathbb{R}$ be a 2π -periodic three-time differentiable function such that $\tilde{f}^{(3)}$ is absolutely continuous; then the Fourier coefficients will, for all j , be bounded from above by

$$|f_j| \leq \frac{c}{|j|^3}, \quad c := \int_{-\pi}^{\pi} |\tilde{f}^{(3)}(x)| dx. \quad (\text{A15})$$

The choice to express the bound in terms of third derivatives is done for convenience only; higher derivatives would have been applicable as well.

3. Application to thermodynamic limits of dispersion relations

These bounds can most conveniently be applied to the situation where one considers instead of an $L \times L$ lattice with toroidal boundary conditions an $L_x \times L_y$ lattice with the same boundary conditions. It is easy to see that by first considering the limit $L_x \rightarrow \infty$ and then the limit $L_y \rightarrow \infty$, one can obtain a rigorous bound on $\lim_{L \rightarrow \infty} S(L)/L$ for the original $L \times L$ lattices at hand. In this way, one can, for each k_y , discuss an appropriate model in the thermodynamic, which simplifies the argument considerably. More precisely put, this is a consequence of the fact that there exists a $\gamma > 0$ such that for $L_x \times L_y$ lattices, for each k_y , the entanglement entropy is shown to satisfy

$$S(k_y, L_x, L_y) \leq \gamma. \quad (\text{A16})$$

Naturally, we can separate the limits of large L_x and L_y in order to simplify the discussion. In light of this discussion, we define for each k_y the functions $\tilde{C}_{\uparrow, \uparrow}(k_y) : (-\pi, \pi] \rightarrow \mathbb{R}$ and $\tilde{C}_{\downarrow, \downarrow}(k_y) : (-\pi, \pi] \rightarrow \mathbb{R}$ as the continuum limits of $\tilde{C}_{\uparrow, \uparrow}$ and $\tilde{C}_{\downarrow, \downarrow}$ for $L_x \times L_y$ lattices in the limit $L_x \rightarrow \infty$. The real-space correlation matrices are then obtained by invoking a Fourier transform, rendering Lemma 1 on the Fourier coefficients of 2π -periodic functions applicable.

4. Discussion of Chern insulator models considered

In this section we discuss the dispersion relations $\tilde{C}_{\uparrow, \uparrow}(k_y)$ for the above model at hand stated in the main text (compare also Fig. 1). Equipped with the above powerful tools, we will see that we can arrive at our conclusion almost without computation. We find that

$$\tilde{C}_{\uparrow, \uparrow}(x, k_y) = 0 \quad (\text{A17})$$

for all $x \in (-\pi, \pi]$ and $\mu < k_y < \pi$. For $k_y \in [-\mu, \mu]$, we find that $x \mapsto \tilde{C}_{\uparrow, \uparrow}(x, k_y)$ is a C^∞ function with a uniformly bounded third derivative. Similarly, one can argue about $\tilde{C}_{\downarrow, \downarrow}(x, k_y)$ since

$$\tilde{C}_{\downarrow, \downarrow}(x, k_y) = 0 \quad (\text{A18})$$

for all $x \in (-\pi, \pi]$ and $\mu < k_y < \pi$. Again, for $k_y \in [-\mu, \mu]$, the function $x \mapsto \tilde{C}_{\downarrow, \downarrow}(x, k_y)$ is a C^∞ function with a uniformly bounded third derivative. The off-diagonal elements of the correlation matrix must decay at least as far as the main diagonal elements, as the correlation matrix is positive semidefinite.

5. Entanglement area laws

With the tools developed, Observation 1 follows immediately: Considering an $L_x \times L_y$ lattice, in the limit $L_x \rightarrow \infty$, for values $\mu < k_y < \pi$, there is no contribution to the entanglement entropy, while for $0 < |k_y| < \mu$ the contribution is bounded from above by a constant: This is a consequence of Theorem 1 and Lemma 1. Using the above argument on the convergence for $L \times L$ lattices defined on the torus, we can conclude that $\mu \rightarrow 0$, $S(L)/L$ converges to zero. This proves the validity of Observation 1.

In fact, an even stronger statement follows, one that is also corroborated by the numerical analysis presented in the main text: The convergence to zero is essentially linear in μ . Precisely put, using the above machinery, it follows that there is a constant $c > 0$ such that

$$\lim_{\mu \rightarrow 0} \frac{1}{\mu} \lim_{L \rightarrow \infty} \frac{S(L)}{L} \leq c. \quad (\text{A19})$$

Intuitively speaking, this follows from the observation that along the k_y direction, the number of contributing terms would shrink linearly in μ , each of which is bounded from above by a constant. With the tools developed, this is a conclusion that can be reached with little calculation.

6. Lower bound

We finally briefly discuss Observation 2, the lower bound to the entanglement entropy. It is clear that any continuous nonzero function $f : (-\pi, \pi] \rightarrow \mathbb{R}^+$ with

$$f(k_y) \leq S(k_y) \quad (\text{A20})$$

will serve as a tool to show that Observation 2 is valid: Consider the partially decoupled situation along the k_y direction. Let $I \subset (-\pi, \pi]$ be an interval in the momentum along the cut with $f(k_y) > \epsilon$ for a suitable $\epsilon > 0$; then in the thermodynamic limit $L_y \rightarrow \infty$, one will encounter a contribution for the entanglement entropy bounded from below by αL for a suitable α . For the function f , several candidates are meaningful. For example, denote with $D^{(AB)}$ the correlation matrix of two pairs of two sites each belonging to the lattice immediately to the left or the right of the cut for the periodic boundary conditions chosen, and let $D^{(A)}$ be the submatrix of $D^{(AB)}$ of only two sites belonging to A . Then

$$S(k_y) \geq f(k_y) := \sum_j 2h(\xi_j^\downarrow(D^{(A)})) - \sum_j h(\xi_j^\downarrow(D^{(AB)})) \quad (\text{A21})$$

(the mutual information), which is always strictly positive unless the state is a product state, and the correlation matrix $D^{(AB)}$ is a continuous function of k_y for the gapped models considered.

- [1] K. v. Klitzing, G. Dorda, and M. Pepper, *Phys. Rev. Lett.* **45**, 494 (1980).
- [2] H. L. Stormer, A. Chang, D. C. Tsui, J. C. M. Hwang, A. C. Gossard, and W. Wiegmann, *Phys. Rev. Lett.* **50**, 1953 (1983).
- [3] R. B. Laughlin, *Phys. Rev. B* **23**, 5632 (1981).
- [4] D. J. Thouless, M. Kohmoto, M. P. Nightingale, and M. den Nijs, *Phys. Rev. Lett.* **49**, 405 (1982).
- [5] R. B. Laughlin, *Phys. Rev. Lett.* **50**, 1395 (1983).
- [6] X.-G. Wen, *Int. J. Mod. Phys. B* **04**, 239 (1990).
- [7] P. W. Anderson, *Basic Notions of Condensed Matter Physics* (Perseus, New York, 1997).
- [8] J. Eisert, M. Cramer, and M. B. Plenio, *Rev. Mod. Phys.* **82**, 277 (2010).
- [9] U. Schollwöck, *Ann. Phys. (NY)* **326**, 96 (2011).
- [10] A. Kitaev and J. Preskill, *Phys. Rev. Lett.* **96**, 110404 (2006).
- [11] M. Levin and X.-G. Wen, *Phys. Rev. Lett.* **96**, 110405 (2006).
- [12] A. Hama, R. Ionicioiu, and P. Zanardi, *Phys. Lett. A* **337**, 22 (2005).
- [13] A. Hama, R. Ionicioiu, and P. Zanardi, *Phys. Rev. A* **71**, 022315 (2005).
- [14] F. D. M. Haldane, *Phys. Rev. Lett.* **61**, 2015 (1988).
- [15] X. Chen, Z.-C. Gu, and X.-G. Wen, *Phys. Rev. B* **82**, 155138 (2010).
- [16] C. L. Kane and E. J. Mele, *Phys. Rev. Lett.* **95**, 226801 (2005).
- [17] C. L. Kane and E. J. Mele, *Phys. Rev. Lett.* **95**, 146802 (2005).
- [18] B. A. Bernevig, T. L. Hughes, and S.-C. Zhang, *Science* **314**, 1757 (2006).
- [19] A. P. Schnyder, S. Ryu, A. Furusaki, and A. W. W. Ludwig, *Phys. Rev. B* **78**, 195125 (2008).
- [20] A. Kitaev, in *Advances in Theoretical Physics: Landau Memorial Conference*, AIP Conf. Proc. No. 1134 (AIP, New York, 2009), p. 22.
- [21] S. Ryu, A. P. Schnyder, A. Furusaki, and A. W. W. Ludwig, *New J. Phys.* **12**, 065010 (2010).
- [22] E. Witten, *Nucl. Phys. B* **223**, 422 (1983).
- [23] X.-L. Qi, T. L. Hughes, and S.-C. Zhang, *Phys. Rev. B* **78**, 195424 (2008).
- [24] H. Li and F. D. M. Haldane, *Phys. Rev. Lett.* **101**, 010504 (2008).
- [25] X.-L. Qi, H. Katsura, and A. W. W. Ludwig, *Phys. Rev. Lett.* **108**, 196402 (2012).
- [26] E. Kapit and E. Mueller, *Phys. Rev. Lett.* **105**, 215303 (2010).
- [27] E. Tang, J.-W. Mei, and X.-G. Wen, *Phys. Rev. Lett.* **106**, 236802 (2011).
- [28] K. Sun, Z. Gu, H. Katsura, and S. Das Sarma, *Phys. Rev. Lett.* **106**, 236803 (2011).
- [29] T. Neupert, L. Santos, C. Chamon, and C. Mudry, *Phys. Rev. Lett.* **106**, 236804 (2011).
- [30] E. J. Bergholtz and Z. Liu, *Int. J. Mod. Phys. B* **27**, 1330017 (2013).
- [31] I. Peschel, *J. Phys. A* **36**, L205 (2003).
- [32] M. Cramer, J. Eisert, and M. B. Plenio, *Phys. Rev. Lett.* **98**, 220603 (2007); M. Cramer, Ph.D. thesis, University of Potsdam, 2007.
- [33] H. Bernigau, M. J. Kastoryano, and J. Eisert, [arXiv:1301.5646](https://arxiv.org/abs/1301.5646).
- [34] A. M. Turner, Y. Zhang, and A. Vishwanath, *Phys. Rev. B* **82**, 241102 (2010).
- [35] L. Fidkowski, *Phys. Rev. Lett.* **104**, 130502 (2010).
- [36] A. M. Turner, Y. Zhang, R. S. K. Mong, and A. Vishwanath, *Phys. Rev. B* **85**, 165120 (2012).
- [37] T. L. Hughes, E. Prodan, and B. A. Bernevig, *Phys. Rev. B* **83**, 245132 (2011).
- [38] This can be achieved by replacing $\mathbf{d}(\mathbf{k}) \mapsto \mathbf{d}(\mathbf{k})/[2\|\mathbf{d}(\mathbf{k})\|]$.
- [39] A. Alexandradinata, T. L. Hughes, and B. A. Bernevig, *Phys. Rev. B* **84**, 195103 (2011).
- [40] W. P. Su, J. R. Schrieffer, and A. J. Heeger, *Phys. Rev. Lett.* **42**, 1698 (1979).
- [41] A. J. Heeger, S. Kivelson, J. R. Schrieffer, and W. P. Su, *Rev. Mod. Phys.* **60**, 781 (1988).
- [42] J. Zak, *Phys. Rev. Lett.* **62**, 2747 (1989).
- [43] Y. Hatsugai, *J. Phys. Soc. Jpn.* **75**, 123601 (2006).
- [44] R. Bhatia, *Matrix Analysis* (Springer, Berlin, 1997).
- [45] In practice, we truncate the lattice in the direction perpendicular to the cut at 30 sites for which the entropy has already converged essentially to machine precision.
- [46] A. Chandran, V. Khemani, and S. L. Sondhi, [arXiv:1311.2946](https://arxiv.org/abs/1311.2946).
- [47] T. B. Wahl, H.-H. Tu, N. Schuch, and J. I. Cirac, *Phys. Rev. Lett.* **111**, 236805 (2013).
- [48] J. Dubail and N. Read, [arXiv:1307.7726](https://arxiv.org/abs/1307.7726).
- [49] B. Beri and N. R. Cooper, *Phys. Rev. Lett.* **106**, 156401 (2011).
- [50] M. Cramer and J. Eisert, *New J. Phys.* **8**, 71 (2006).
- [51] F. G. S. L. Brandao and M. Horodecki, *Nat. Phys.* **9**, 721 (2013).
- [52] A. R. Its, B.-Q. Jin, and V. E. Korepin, [arXiv:quant-ph/0606178](https://arxiv.org/abs/quant-ph/0606178).
- [53] Y. Katznelson, *An Introduction to Harmonic Analysis*, 3rd ed., Cambridge Mathematical Library (Cambridge University Press, Cambridge, 2004).